RSC Advances

Highly dispersed platinum nanoparticles supported on silica as catalyst for hydrogen production

Journal:	*RSC Advances*
Manuscript ID:	RA-ART-08-2014-009341.R1
Article Type:	Paper
Date Submitted by the Author:	23-Sep-2014
Complete List of Authors:	Khdary, Nezar; King Abdulaziz city for Science and Technology, Ghanem, Mohamed; King Saud University, Chemistry Department

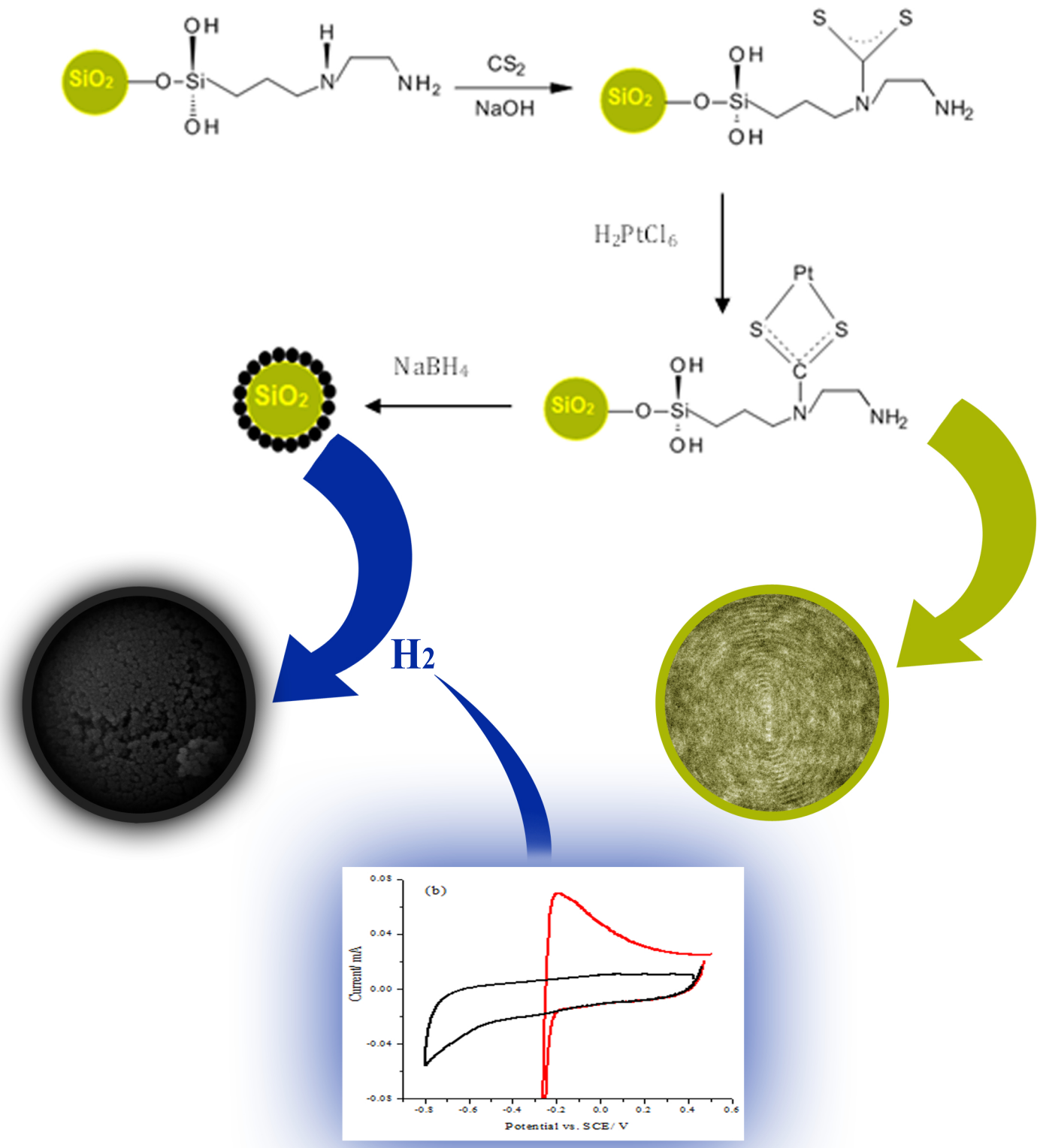
SiO2
OH
H
NH2
CS2
NaOH
S
S
H2PtCl6
Pt
C
NaBH4
H2
(b)
Current/ mA
Potential vs. SCE/ V

Highly dispersed platinum nanoparticles supported on silica as catalyst for hydrogen production.

Nezar Khdary[a,*] and Mohamed A. Ghanem[b]

King Abdulaziz City for Science and Technology, P O Box 6086 Riyadh 11442, Kingdom of Saudi Arabia; Tel: +966555515619.

[b]*Chemistry Department, College of Science, King Saud University, Kingdom of Saudi Arabia.*

Abstract

Synthetic approach is developed to produce highly disperse, low loading (3.28 wt. %) Pt nanoparticles incorporated silica (Pt-NP-S) with average diameter of 3.5 nm using economical and simple surface chemical modification and reduction processes. This was achieved by using silica modified by dithiocarbamate functional groups treated with solution of hexachloroplatinic acid and followed by chemical reduction to produced Pt nanoparticles incorporated silica support. The physicochemical characterizations of the Pt nanoparticles incorporated silica were performed by elemental analysis, FTIR, TGA, chemisorption analysis and transmission electron microscopes. The results show that the Pt nanoparticles were uniformly distributed throughout the silica support with Pt loading of 3.2 wt. % and particle diameter range from 2 to 5 nm. The electrocatalytic activity and stability for hydrogen evolution reaction was evaluated using cyclic voltammetry and chronoamperometry. At more negative potential than the hydrogen evolution of -250 mV vs. SCE, the catalyst shows high activity for hydrogen evolution with current density of 11.90 A/g_{Pt} mV. The preparation procedure is simple and favorable for variety of metal nanoparticles synthesis for catalysis applications.

Introduction

The immobilization of functional groups, metal complexes and nanoparticles to the silica surface has attracted great interest due to their uses in many applications, such as chromatography [1, 2], extraction of cations from aqueous and non-aqueous solvents [3, 4, 5] catalytic or ion-exchange reactions [6, 7, 8,] and chemical sensors [9, 10]. The amine functional groups immobilized on silica gel surfaces are widely used for adsorbing metal ions from aqueous and non-aqueous solutions and capturing CO_2 while thiol functional groups used mainly to adsorb heavy metal ions [11, 12]. Dithiocarbamate and derivatives are examples of bi-functional chelating agent that contains sulfur and nitrogen functional groups and exhibit various preferences for binding with different metal ions [11,13]. In addition, these silica based modified materials show good chemical stability and high selectivity and sorption capacity.

Silica surface modification can be achieved either by physical adsorption or chemical grafting of functional groups. In chemical coupling, the functional groups are covalently bonded by direct reaction of organosilanes, thiol or alkyl groups to the silica surface [11]. This chemical bonding of functional groups to silica surface offers a unique advantage due to the strong molecules covalent bonding to the substrate, resistive to the chemical change and can be used in harsh conditions.

Metal nanoparticles (MNPs) are clusters containing tens to thousands of metal atoms and their sizes are vary between one to tens of nanometers [14]. They are very attractive catalysts due to their large surface area and smaller size which results in superior catalytic activity [15, 16, 17, 18]. There are many research work focus on

the metal nanoparticles loaded on different supports for heterogeneous catalyst applications in many organic and inorganic reactions [19, 20, 21], industrial processes [22, 23, 24] and in particular for selective oxidation reactions [25, 26]. The incorporation of metal nanoparticles into support matrix such as silica is carried out by variety of methods, such as wet impregnation, ion exchange and chemical surface modification [2-4, 27, 28, 29, 30, 31, 32, 33]. In the surface modification method, the metal precursors (ions) are attached to the support surface through pre-attached functional groups followed by chemical reduction to form metal nanoparticles incorporation composite [34, 37]. Platinum nanoparticles having diameters ranging from 3 to 10 nm have been widely used as a catalyst in particular for fuel cells, due to their large surface area and excellent enhanced catalytic properties [35, 36]. To obtain efficient metal nanoparticle catalyst, it is necessary to have the highest possible degree of metal dispersion, smaller particle size and low loading, especially, for expensive noble metal such as platinum. This can be achieved by fixing the metal cations into a rigid support through organic ligand attachment subsequently execute the chemical reduction to produce the supported metal nanoparticles. This chemical preparation principal should be applicable for any reducible metal ion fastened to any support with appropriate linker. Very recently we demonstrated the accomplishment of the above aim and prepared nanocomposites composed of Cu, Fe, Ag and Au and ions incorporated to ethylene diamine and mercaptopropyl modified silica which showed enhancement for CO_2 sequestration capacity [34, 37].

In this work and using above strategy we demonstrate the preparation and characterization of Pt dithiocarbamate complex (Pt-DTC-S) and Pt nanoparticles (Pt-NP-S) supported silica gel. Silica surface was firstly modified with dithiocarbamate functional groups using N-[3-(trimethoxysilyl)propyl]ethylendiamin and CS_2 coupling agents. Then the modified silica is treated with solution of hexachloroplatanic acid to form the Pt dithiocarbamate complex. The attached metal ions finally are reduced into metal nanoparticles using sodium borohydride reducing agent. To the best of our knowledge this is the first work to use the dithocarbamate linker to immobilize Pt nanoparticles into the silica surface [USA Patent 502628570]. The surface modification method has the advantages of binding the metal ions into the active surface functional groups which achieve minimal nanoparticle aggregation and produce low loading and uniform particle distribution. The physicochemical properties of the resulting Pt-DTC-S and Pt-NP-S are systematically characterized by CHN elemental analysis, FTIR, N_2 adsorption isotherm, EDX, TGA, chemisorption analysis and TEM. The electrocatalytic activity of the Pt-NP-S for hydrogen evolution is also investigated by cyclic voltammetry and chronoamperometry. This new low cost material could lead to new revolution in hydrogen production catalyst.

Experimental

Chemicals

Silica gel (particle size 40-60 μm, surface area = 409 m^2/g, pore size 60 Å) was purchased from ACROS Organic (USA). Toluene, ammonia and ammonia buffer solutions were obtained from BDH (Europe) and methanol and isopropanol obtained from (Prolabo, Europe). N-(3-(Trimethoxysilyl propyl) ethylenediamine (Acros, USA), sodium borohydride and hexachloroplatanic acid from (BDH, UK) and carbon disulfide was obtained from LOBA CHEMIE, India).

Characterizations

Fourier transform infrared (FTIR) spectra were recorded at room temperature on powder samples using ALPHA BRUKER spectrophotometer and CHN analysis was carried out using 2400 CHN analyzer (Perkin Elmer, Series II CHNS/O Analyzer). The BET surface area was measured using nitrogen physisorption at 77 °K using Micromeritics ASAP 2010P and the sample was degasing using the same system at 120 °C for overnight. Platinum nanoparticles dispersion was assessed by carbon monoxide chemisorption at 35 °C using Micromeritics ASAP 2020C. The evacuation was carried out using He at 110 °C for 30 min flowed by H_2 for 10 min at 100 °C and for 120 min at 350 °C.

Powder X-Ray diffraction (XRD) analysis was executed using Bruker a D8 advanced DaVinci diffractometer configured with Lynxeye Xe detector and 2.2 KW Cu. The EDX analysis was performed using the X-ray detector integrated into scanning electron microscope (FEI Nova 200 dual-beam Scanning Electron Microscope). Transmission electron microscopic (TEM) investigations were carried out using a JEM2010 electron microscope at 200 KV. The electrochemical measurements were accomplished using BioLogic VSP Potentiostat with EC-Lab V10.21 software. Conventional three-electrode cell was used with a 1.0 cm^2 platinum gauze counter electrode and saturated calomel as reference electrode (BAS Inc., Japan). The working electrode was 3.0 mm diameter glassy carbon (GC, HTW, Germany) sealed in glass and connected to copper wires using indium. Prior to the electrochemical characterization the catalyst was activated by heating at 200 ^oC in air atmosphere for 1 hour then 10.0 mg of Pt nanoparticles supported silica was suspended by sonication in 1.0 ml isopropanol mixed with 10 µl of 5.0 wt.% nafion. A 15 µl of the catalyst suspension was loaded on GC carbon disk electrode and left to dry in air at room temperature.

Synthesis of Pt dithiocarbamate complex and Pt nanoparticles supported silica.

The silica particles were firstly modified with N-(3-(Trimethoxysilyl propyl) ethylenediamine by transferring 150 mL of dry toluene into a 250 mL round-bottom flask fitted with a reflux condenser. A 5.0 g of silica gel was dispersed in toluene by agitation and heated to 90 °C. After the temperature had stabilized, 2.0 mL of N-[3-(trimethoxysilyl)propyl] ethylenediamine was slowly added to the flask and the reaction was carried out under nitrogen atmosphere for 6 hours then cooled down to room temperature. The diamine modified silica was separated by centrifuging and rinsed thoroughly with toluene and dried for overnight under vacuum. The modification of silica with bis-dithiocarbamate was executed by adding 100 mL of deionized water and 2.0 mL NaOH solution (0.1 M) into a 500 mL three necked round bottomed flask. A 5 g of the diamine modified silica was added to the reaction flask followed by 8 mL of isopropanol. After 10 minutes of sonication, 8 mL of carbon disulfide was added and the reaction was left to proceed under nitrogen at 20 ^oC for 1 hour. The product was centrifuged and the white precipitate was rinsed four times with isopropanol until no absorbtion was seen at 265 nm for CS2. The product was dried in a vacuum desiccator and stored under nitrogen at 4 °C prior to use.

The synthesis of platinum complex supported silica (Pt-DTC-S) was carried out by transferring 500 mg of bis-dithiocarbamate modified silica into 40 ml glass vial and 5.0 ml of H_2PtCl_2 solution (1.0 M) was added and shaken for 1 hour. The excess of metal ions solution was removed by washing the sample with deionized water several times until no absorption was observed for the effluent at 300 nm. The color of bis-dthiocarbamate-silica was changed from white to yellow after complexation with platinum ions. The platinum nanoparticles supported silica (Pt-NP-S) was prepared by transferring 150 mg of (Pt-DTC-S) to 40 ml glass vial which has inlet /outlet

needle and 5 ml of fresh prepared $NaBH_4$ (2.0 M) was slowly added to the vial and left for 30 minutes until the metal dark color was observed. The product was rinsed several times with ultra-pure deionized water and kept under nitrogen to dry in desiccator. For comparison, a control sample (Pt-unmodified-silica) was prepared by soaking of 500 mg unmodified silica with 5.0 ml of H_2PtCl_2 solution (1.0 M) for overnight with shaking. Then the excess of the H_2PtCl_2 solution was removed and the Pt ions reduction using same procedure reported above.

Results and Discussion

Complex of Pt bis-dithiocarbamate and Pt nanoparticles supported silica.

Pt dithiocarbamate and Pt nanoparticles supported silica were performed as shown in scheme 1. The immobilization of the N-[3-(trimethoxysilyl)propyl]ethylenediamine followed by attachment of CS_2 to silica particles was performed as described above in the experimental part. The dithiocarbamate modified silica was treated with H_2PtCl_6 to produce Pt ions bonded silica surface through the bis-dithiocarbamate linker. The silica modified Pt complex was reduced by $NaBH_4$ to produce Pt-nanoparticles loaded on silica.

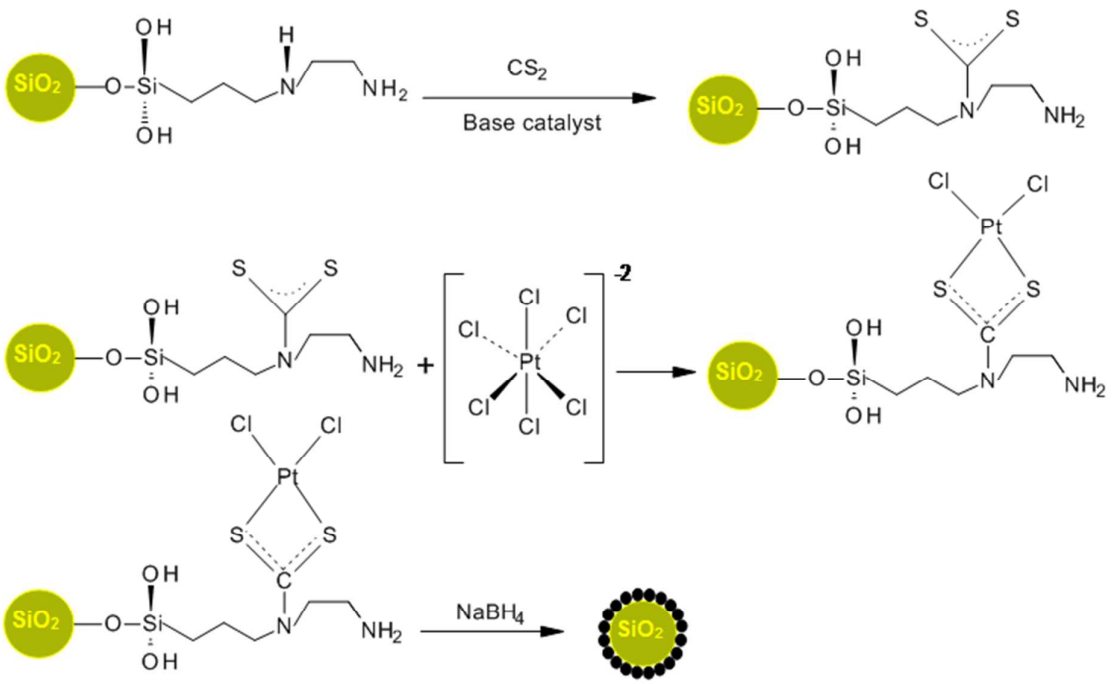

Scheme 1 Modification of silica with dithiocarbamate, complexation with Pt ions and reduction to Pt nano particles supported silica surface.

Fig. 1 shows the optical images for silica (a) and modified silica with bis-dithiocarbamate (b) modified silica after treated with H_2PtCl_6 solutions (c) and after reduction with $NaBH_4$ (d). For comparison a control experiment using unmodified silica was performed at the same condition and is shown in Fig. 1a. Clearly, after treatment of bis-dithiocarbamate modified silica with H_2PtCl_6 solution, its color changes from white to yellow. The coloration of silica particles is a qualitative indication on the formation of Pt –bis-dithiocarbamate complex on

silica surface. This complex is stabilized when adsorbed on solid surface and also may have cross linkage and internal polymerization due to the presence of S and N-chelated groups [13]. Finally the silica immobilized Pt complex is chemically reduced in aqueous solution using sodium borohydride reducing agent to produce the metal nanoparticles incorporated silica support. Optical images in Fig. 1d shows the Pt-dithiocarbamate changed into black after the reduction with $NaBH_4$ which quantitatively indicates of the formation of Pt nanoparticles.

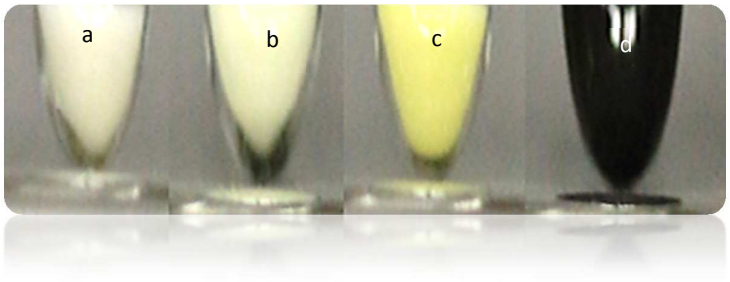

Fig. 1 Optical images of (a) dried plain silica, (b) DTC-S, (c) DTC-S Pt-complex, (d) DTC-S Pt- NP-S.

Fig. 2 shows the FTIR characterization of silica modified with dithiocarbamate and after the formation of Pt complex and Pt nanoparticles. The FTIR spectra show the existence of the bands at approximately 1097, 802, 460 cm^{-1} which assigned to the stretching, bending and rocking modes of the Si–O-Si bonds of silica particles [38, 27**Error! Bookmark not defined.**].

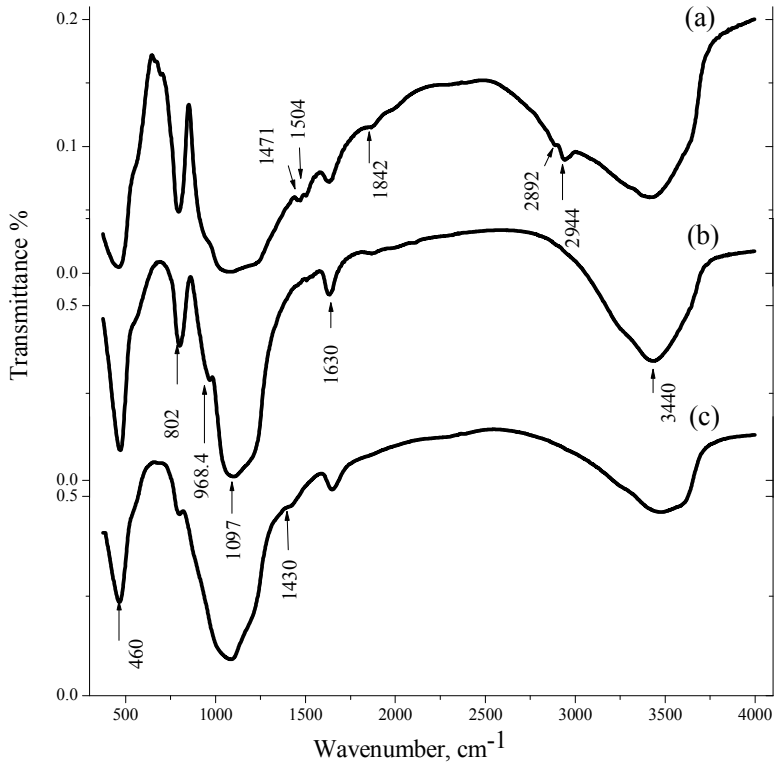

Fig. 2. FTIR spectrum for (a) dithiocarbamate modified silica, (b) Pt-dithiocarbamate-silica and (c) Pt-nanoparticles-silica.

The band near 1630 cm^{-1} corresponds to the bending mode of OH groups of adsorbed water and the broad band centered at 3440 cm^{-1} assigned to adsorbed water and H bonded silanol OH groups [39]. The IR spectrum in Fig. 2a shows the band at 1504 is characteristic for C-S stretching and the C–H stretching vibrations of propyl chain is observed around 2892 and 2944 cm^{-1}. After the formation of Pt dithiocarbamate complex the FTIR spectrum shows a shift to the right (Fig.2.b). The shoulder at about 3415 cm^{-1} most likely corresponds to the symmetric stretching modes of NH_2 groups [40]. However, after the reduction with $NaBH_4$ the peaks at 1471 and 1504 cm^{-1} were disappearing (Fig.2 c) this may due to $NaBH_4$ cause partial reduction of thiol to H_2S. The shoulder at 1430 is appear only after reduction and may associated with Pt-Nanoparticles on silica surface after the reduction of Pt complex.

Table 1 shows the elemental (CHNS) analysis for plain silica particles and after modification with dithiocarbamate. The analysis clearly show an increase in C, H, N and S elements contents which confirms the attachment of the dithiocarbamate functional groups to the silica surface. From the CHNS analysis of dithiocarbamte modified silica the estimated nitrogen loading equals to 0.55 mmol/g while sulfur content reaches 0.178 mmol/g. After the attachment and reduction of Pt ions, the nitrogen content was slightly decreased while sulfur content was significantly reduced. In addition a smile of H_2S was evolved during treating the Pt-DTC-S with sodium borohydride which apparently due to the reduction of dithiocarbamate to H_2S.

Table 1 Elemental analysis for plain silica, (DTC–S) and Pt-NP-S.

Elements wt. %	Plain silica	Silica-DTC	Pt-DTC-S	Pt-NP-S
C%	0.14	1.92	1.58	1.50
H%	0.89	0.90	1.09	0.95
N%	0.06	0.78	0.70	0.69
S%	0.02	0.57	0.48	0.33

Fig. 3 shows the thermal gravimetric analysis for the silica gel modified with dithiocarbamate over temperature range from 25 to 700 ^{o}C in air. The weight loss observed between room temperature and 100 ^{o}C corresponds to the release of the physically adsorbed water and it was about 4.5 wt.%.

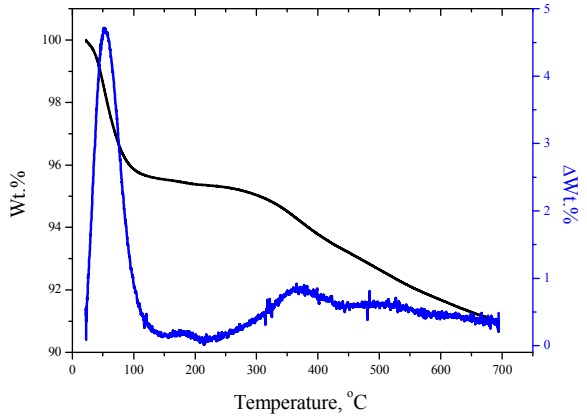

Fig. 3 Thermogravimetric analysis (TGA) for diamine-thiocarbamate modified silica, during heating in air.

On further heating the decomposition of attached dithiocarbamate linker took place over the temperature range from 250 to 600 ^{o}C. Within this heating region the accompanied weight loss was about 0.6 wt.% due to the dithiocarbamate group degradation which is consistence with the reported literatures [41].

X-ray diffraction pattern of Pt-nanoparticles-dithiocarbamate-silica is shown in Fig.4. The broad diffraction peak with high intensity at around 2θ shows the signal from the amorphous silica gel. The other four small diffraction peaks with relatively low intensities can assigned to Pt (fcc) diffraction planes of (111), (200), (220) and (311). The relatively broad and low intensity of the diffraction peaks indicates on small crystalline size and loading of the Pt nanoparticles.

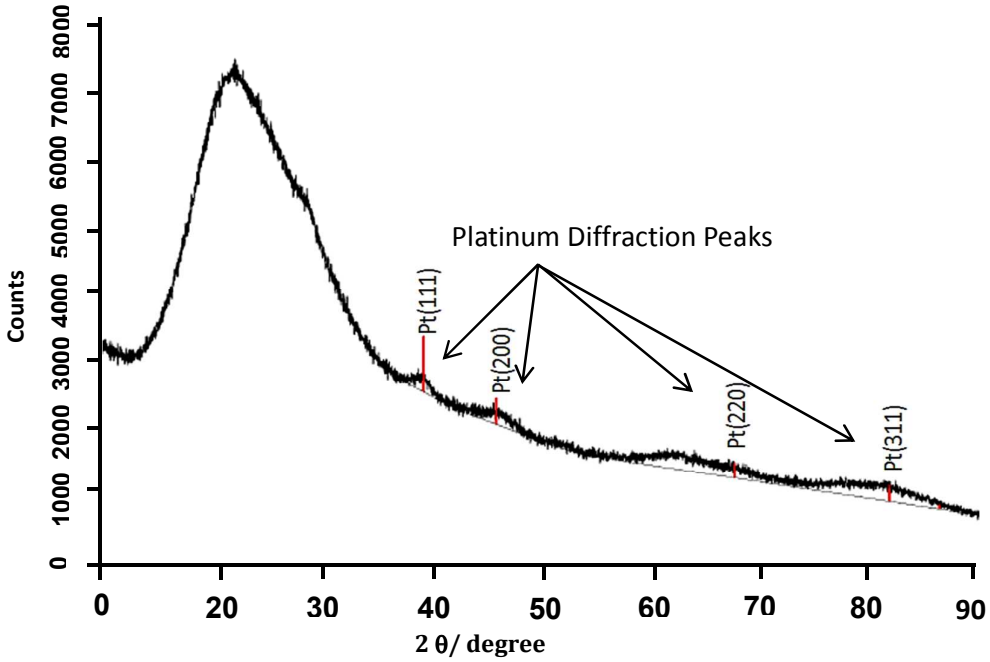

Fig. 4 X-ray diffraction of Pt nanoparticles loaded on silica support.

Fig. 5 shows the energy dispersive X-ray spectrum from for Pt nanoparticle-decorated silica. The O(K) and Si(K) peaks are from the silica support. The peak at around 2.1 keV is assigned to Pt(M) and it can be seen from the inset table the Pt content reaches 0.995 wt% and for sulfur is 0.92. This supports that the low loading of Pt nanoparticles on the silica particles.

Fig. 6 shows the transmission electron microscope images at lower and higher resolutions for the Pt metals nanoparticles supported on dithiocarbamate-silica (Pt-NP-S). The Pt nanoparticles show homogeneous dispersion throughout the silica support and display spherical shapes nanoparticles.

The nanoparticles exhibit a narrow size and the average size distribution is 3±1.5nm as shown in the inset histogram in Fig. 6b. The Pt nanoparticles diameter obtained her is much smaller than the diameter of 10 to 35 nm which obtained for Pt nanoparticles supported mesoporous silica (MCM-41) and incorporated by wetness and in situ impregnation [42]. Moreover, it is the same as the particle size obtained by the coupling agent-assisted sol–gel method [43]. Obviously the presence of dithiocarbamate functional groups provides well dispersed metal nanoparticles and prevents the migration and aggregation of Pt nanoparticles over the silica surface during synthesis process.

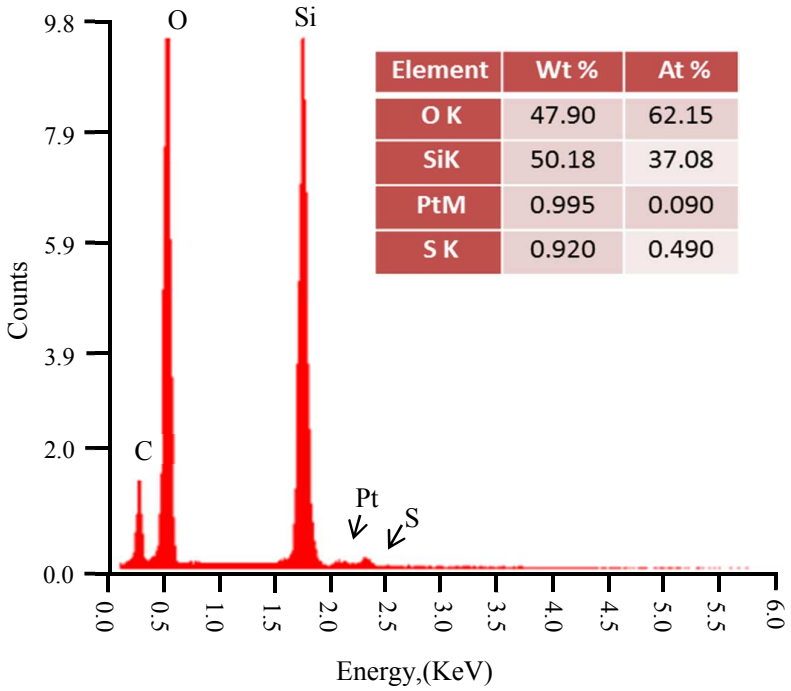

Element	Wt %	At %
O K	47.90	62.15
SiK	50.18	37.08
PtM	0.995	0.090
S K	0.920	0.490

Fig. 5 Energy dispersive X-ray spectrum of Pt nanoparticles loaded on silica support.

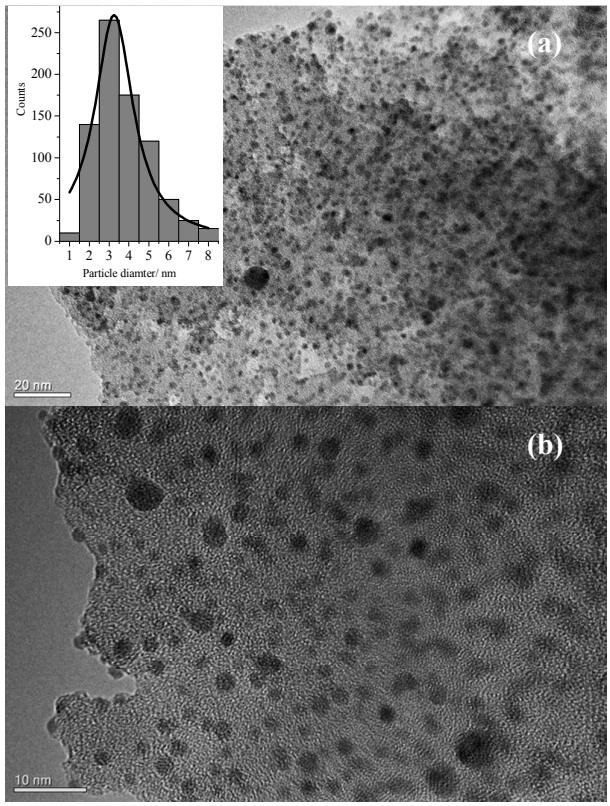

Fig.6. TEM images for Pt nanoparticles supported silica gel, (a) lower, and (b) higher magnification. The inset shows the particle size distribution histogram.

The chemical adsorption isotherm of Pt nanoparticles supported silica was investigated to reveals more information about the active surface and platinum dispersion. Fig. 7 shows the CO chemisorption analysis of the Pt-NP-S catalyst. The platinum loading measured from the adsorption isotherm is equal to 3.28 wt. % with metallic surface area of 8.1 m^2/g_{Pt}.

The Pt nanoparticles loading can be estimated at 0.168 mmol/g of silica that is very consistent with the value of 0.178 mmol/g of sulfur loading and indicates that Pt ions bonded to dithiocarbamate with ratio of 1: 1 on silica surface.

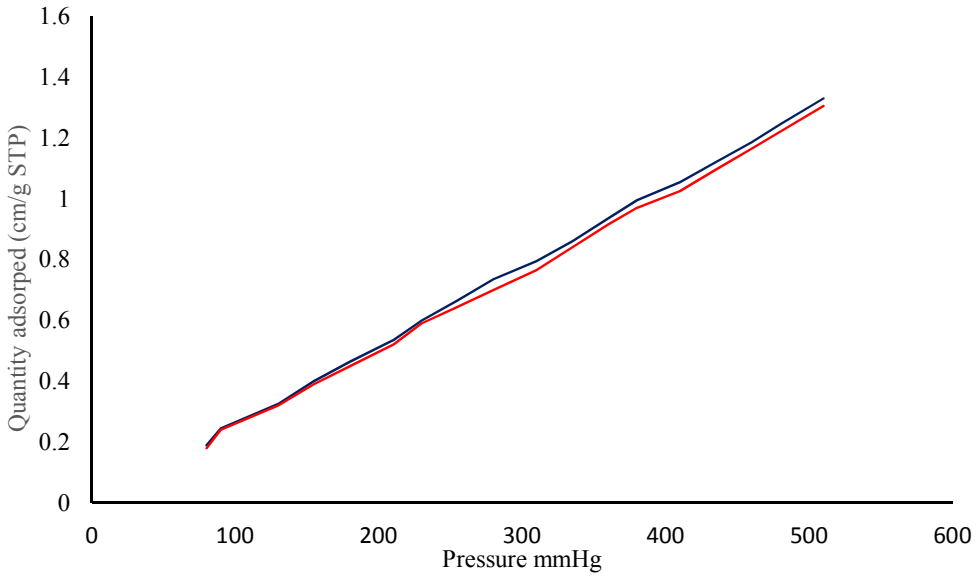

Fig. 7: The chemisorption analysis of CO on Pt-NP-S.

Electrocatalytic activity of Pt-S toward hydrogen evolution reaction.

The preliminary catalytic activity and stability of Pt-NP-S catalyst toward hydrogen evolution reaction HER in 1.0 M H_2SO_4 were studied by cyclic voltammetry and chronoamperometry. Fig. 8a shows the multi-cyclic voltammetry curves (20 cycles) at 50 mV s^{-1} for the Pt nanoparticles silica catalyst (red line, total Pt loading about 0.5 μg) and Pt-bare-silica (black line) in 1.0 M H_2SO_4. For Pt-NP-S catalyst, the HER onset potential occurs at about - 0.225 V vs. SCE while for Pt-bare-silica at -0.325 as indicated by an abrupt increasing in the cathodic current as shown in Fig. 8b. In potential region more negative than -0.25 V vs. SCE, the Pt-NP-S catalyst shows high activity for hydrogen evolution with current density of 11.9 A/g_{Pt} mV which is much higher than that reported for Pt nanoparticles incorporated by wetness and in situ impregnation into mesoporous silica (MCM-41) [42] . In case of the Pt-bare-silica catalyst, the HER current was very small at more negative potential and the catalyst does not show any hydrogen desorption peak during the reverse scan (black line Fig. 8b). The electrochemical active area (EAA) for the Pt-NP-S calculated from the charge of hydrogen desorption region (Fig. 8b) reaches about 7.8 m^2/ g_{pt} which is very consistent with the metallic surface area of 8.1 m^2/g_{Pt} measured by CO chemisorption analysis. The HE current density increases by increasing the H_2SO_4 concentration and the scan rate (supplementary information Fig. 1 and 2).

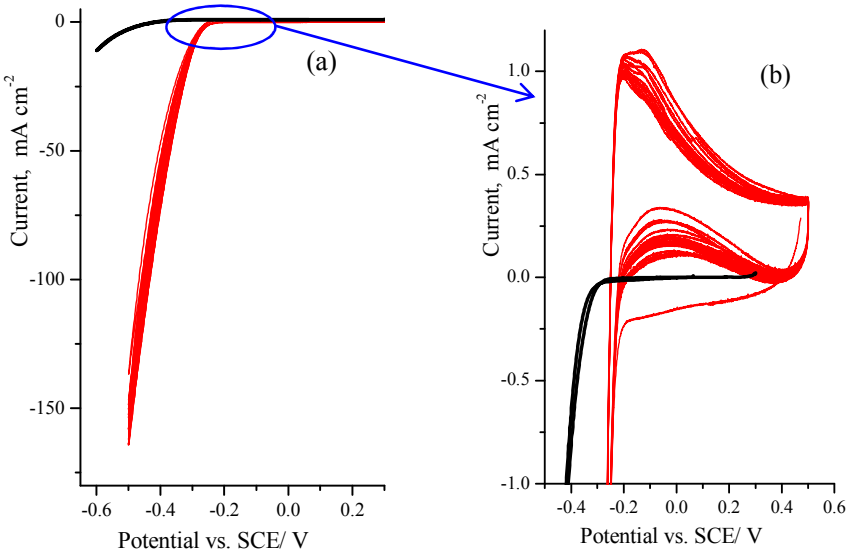

Fig. 8 (a) cyclic voltammetry at 50 mVs^{-1} for (red line) Pt-NP-S and (black line) Pt-bare silica loaded on GC electrode in 1.0 M H_2SO_4. (b) Enlarged area of cyclic voltammetry in (a) showing the hydrogen onset evolution potential and desorption peak.

The long-term stability of the Pt-NP-S catalyst for hydrogen evolution reaction was evaluated by multi-cycling and chronoamperometry. Fig. 9a shows the cyclic voltammetry for Pt-NP-S in 1.0 M H_2SO_4 for the first and the 100 cycles. We can see catalyst is stable for more than 100 cycles and hydrogen evolution current increases with successive cycling as well as the onset potential of HER shifts to more positive potential due to the catalyst surface cleaning by hydrogen evolution. Fig. 9b shows the chronoamperometry for Pt-NP-S catalyst in 1.0 M H_2SO_4 measured at different reduction potentials. The results in the chronoamperometry show that at the start, the current is superimposed before it drops rapidly due to double layer charging current and then gradually decays until approaching steady state that limited by the diffusion of hydrogen ions. The result shows that after 3000 s, HE current density at Pt-NP-S is about five times greater than that at Pt-unmodified silica catalyst which confirms the good performance and stability of Pt-NP-S catalyst.

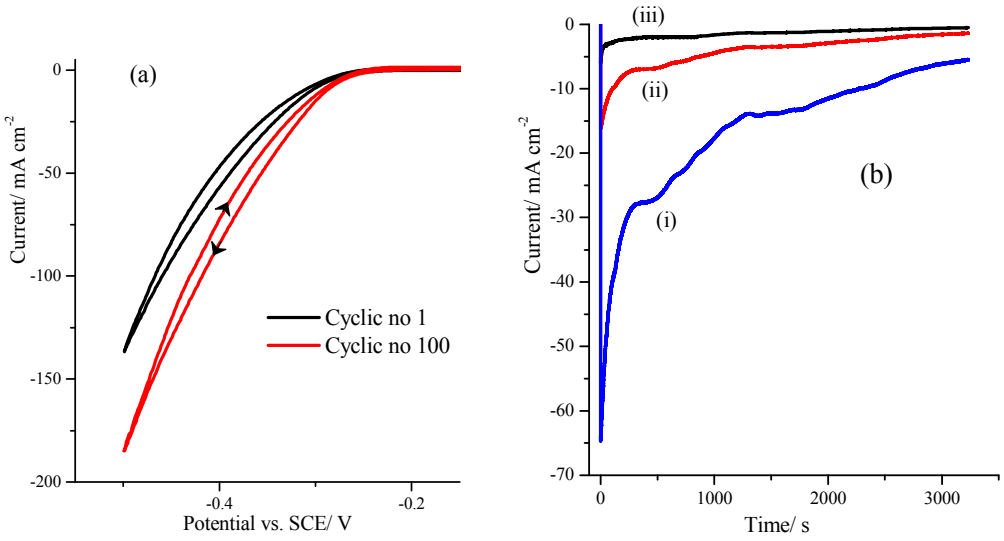

Fig. 9 Chronoamperometry for Pt-NP-S catalyst electrode in in 1.0 M H_2SO_4 at (i) -400 mV, (ii) -300 and (iii) Pt-bare silica at -400 mV vs. SCE.

In comparison of the HER catalytic activity, table 2 listed the specific catalytic activities for some commercial Pt based catalysts reported in literatures. The specific catalytic activity of our Pt-NP-S catalyst for HER (at - 0.5 V vs. SCE in 1.0 M H_2SO_4) reaches up to 140 mA/ cm^2 which is much higher than the commercial Pt carbon-supported catalysts given that the experimental conditions and the platinum loading percentage [44]. In addition the Pt-NP-S catalytic activity is significantly higher than the activity of Pt catalyst prepared by impregnation into mesoporous silica [42] and it is good as the activity obtained for platinum hollow nanospheres immobilized on graphene nanosheet [45].

Table 2. Comparison of the HER onset potential and specific activity of Pt-NP-S catalyst with Pt based catalysts reported in literature.

Catalyst	Onset potential, mV vs. SCE	Specific activity mA/cm^2	Reference
Pt foil[a]	-246	109	44
20 wt% Pt/C E-Tek[a]	-246	55	44
5 wt% Pt/MCM-41[b]	-240	3.0	42
Pt nanosphers/graphene[c]	-370	110	45
Pt hollow nanosphers/graphene[c]	-230	200	45
Pt-NP-S catalyst[c]	-225	140	This work
Pt-unmodified silica	-0.325	2.0	This work

[a] Current measured at E = - 0.3 V vs. NHE in 1.0 M H_2SO_4, scan rate 2.0 mVs^{-1}; [b] E = -0.5 V vs. SCE, in 0.5 M H_2SO_4, [c] E = -0.5 V vs. SCE in 1.0 M H_2SO_4, scan rate 50 mVs^{-1}.

The effect of H_2SO_4 concentration on the hydrogen evolution activity at Pt-NP-S catalyst was performed by cyclic voltammetry and shown in Fig. 10 (a) below. The cyclic voltammograms show by increasing the concentration of H_2SO_4, the HE current density increases. In addition, the effect of scan rates on hydrogen evolution also demonstrates same trend as shown in Fig. 10 (b).

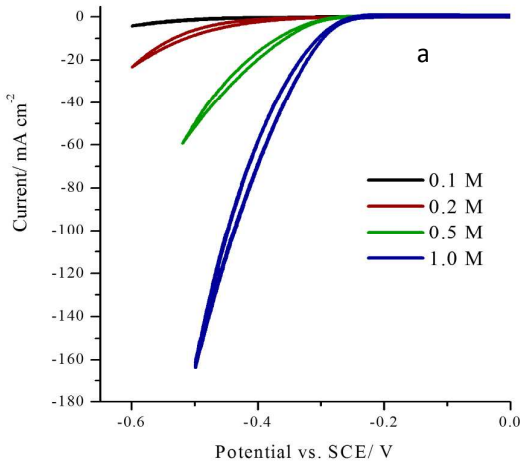

Fig. 10(a) cyclic voltammetry at 50 mVs^{-1} for Pt nanoparticles supported silica (Pt-NP-S) loaded on GC electrode in different concentration of H_2SO_4.

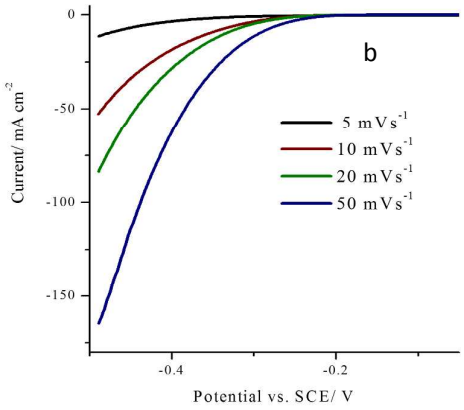

Fig. 10(b) Effect of scan rate on hydrogen evolution reaction at Pt-NP-S catalyst loaded on GC electrode in in 1.0 M H_2SO_4.

Conclusion

In summary, synthetic method is developed to produce highly disperse and low loading (3.28 wt. %) silica supported Pt nanoparticles (Pt-NP-S) using low cost and simple surface chemical modification. Silica surface was chemically grafted with dithiocarbamate functional groups by treating with silane coupling agent of N-[3-(trimethoxysilyl) propyl]ethylendiamin and CS_2. The Pt ions then attached to the dithiocarbamate modified silica and followed by chemical reduction to produce the Pt nanoparticles. Physicochemical analysis and characterizations prove that the metal nanoparticles show a uniform shape and high dispersion with particle diameter in range from 2.0 to 5.0 nm. The immobilization of Pt ions into silica surface by dithiocarbamate ligand was very effective and enhanced the Pt dispersion as shown by TEM characterization. At applied potential more negative than -250 mV vs. SCE, the Pt nanoparticles supported silica catalyst exhibit very high and stable electrocatalytic activity for hydrogen production with mass activity of 11.9 A/g_{Pt} mV. The method is very simple and allows for easy and low cost preparation for effective electrode based on the cheap silica substrate. Additional studies are currently in progress to apply this method to synthesis other metals and bimetallic nanoparticles incorporated silica for catalysis applications.

Acknowledgement

This work is funded by King Abdulaziz City for Science and Technology (KACST) project number 593-32.

References.

[1] Fryxell, GE. The synthesis of functional mesoporous materials. Inorg Chem Commun 2006; 9:1141–1150

[2] Verzele M, Van de Velde N. Anthracene silica gel, a new polycyclic-aromatic-bonded stationary phase for HPLC. Chromatographia 1985; 20: 239-241.

[3] Khdary NH, Howard A. G. New solid-phase-nanoscavenger for the analytical enrichment of mercury from water. Analyst 2011; 136:3004–3009

[4] Lessi P, Dias Filhob NL, Moreira J C, Campos TS. Sorption and pre-concentration of metal ions on silica gel modified with 2,5-dimercapto-1,3,4-thiadiazole. Anal Chimica Acta 1996; 327:183-190.

[5] Dias Filho NL, Gushikem Y, Polito WL, Moreira JC, Ehirim EO. Sorption and preconcentration of metal ions in ethanol solution with a silica gel surface chemically modified with benzimidazole. Talanta 1995; 42:1625-1630.

[6] Khdary NH, Gassim A. E, Howard A. G. Scavenging of benzodiazepine drugs from water using dual-functionalized silica nanoparticles. Analytical Methods 2012; 4:2900-2907

[7] Gushikem Y, Moreira WC. Exchange properties of silica gel functionalized with pyridinium ionOriginal Research Article. Colloids Surf 1987; 25:155-165.

[8] Jiang C, Hara K, Fukuoka A. Low-Temperature oxidation of ethylene over platinum nanoparticles supported on mesoporous silica. Angew Chem Int Ed 2013; 52:1-5.

[9]Khdary NH, Extraction of Di-Methyl Phthalate Using Smart Nanoscavengers. Advanced Materials Research. 2014; 950: 29-32.

[10] Fernandes JR, Kubota LT, Gushikem Y, Oliveira NG. A New Sensor for perchlorate Ion. Anal. Lett. 1993, 26, 2555-2563.

[11] Jal PK, Patel S, Mishra BK. Chemical modification of silica surface by immobilization of functional groups for extractive concentration of metal ions. Talanta 2004; 62:1005–1028

[12] Howard AG, Khdary NH. Nanoscavenger based dispersion preconcentration; sub-micron particulate extractants for analyte collection and enrichment. Analyst 2005;130:1432–1438.

[13] Faraglia G, Fedrigo MA, Sitran S. Palladium(II) and platinum(II) complexes of dithiocarbamates and L-methioninol. Trans Metal Chem 2002; 27: 200–206.

[14] Feldheim DL, Foss CA. Metals nanoparticles, synthesis, characterization and applications. Switzerland : Marcel Dekker AG; 2002.

[15] Bell AT. The Impact of Nanoscience on Heterogeneous Catalysis. Science 2003; 299:1688-1691.

[16] N. Zheng N, Stucky DG.A general synthetic strategy for oxide-supported metal nanoparticle catalysts. J Am Chem Soc 2006; 128:14278–14280.

[17] Formo E, Lee E, Campbell D, Xia Y. Functionalization of electrospun TiO_2 nanofibers with Pt nanoparticles and nanowires for catalytic applications. Nano Lett 2008;8: 668–672.

[18] Xie XW, Li Y, Liu ZQ, Haruta M, Shen W J. Low-temperature oxidation of CO catalysed by Co_3O_4 nanorods. Nature 2009; 458: 746-749.

[19] Scott S L, Crudden CM, Jones CW. Nanostructured catalysts. New York: KLUWER Academic Publishers; 2005.

[20] Blackman JA. Metallic Nanoparticles, Handbook of metal physics. Amsterdam: Elsevier; 2009.

[21] Astruc D. Nanoparticles and catalysis. Weinheim : WILEY-VCH Verlag GmbH & Co;2008.

[22] Hashmi ASK, Hutchings GJ. Gold catalysis. Angew Chem Int Ed 2006;45: 7896–7936.

[23] Corma A, Garcia H. Supported gold nanoparticles as catalysts for organic reactions. Chem Soc Rev2008;37:2096-2126.

[24] Yu N, Ding Y, Lo A, Huang S, Wub P, Liu C, Yin D. Fu Z et al. Gold nanoparticles supported on periodic mesoporous organosilicas for epoxidation of olefins: Effects of pore architecture and surface modification method of the supports. Micropor Mesopor Mater 2011;143:426–434.

[25] Min BK, Friend CM. Heterogeneous gold-based catalysis for green chemistry: low-temperature CO oxidation and propene oxidation. Chem Rev 2007; 107: 2709 2724.

[26] Pina CD, Falletta E, Prati L, Rossi M. Selective oxidation using gold. Chem Soc Rev 2008; 37: 2077-2095.

[27] Gu J, Shi J, You G, Xiong L, Qian S, Hua Z, Chen H. Incorporation of highly dispersed gold nanoparticles into the pore channels of mesoporous silica thin films and their ultrafast nonlinear optical response. Adv Mater 2005; 17:557.

[28] Cui F, Hua Z, Wei C, Li J, Gao Z, Shi J. Highly dispersed Au nanoparticles incorporated mesoporous TiO2 thin films with ultrahigh Au content. J Mater Chem 2009; 19:7632-7637.

[29] Chen H, Shi J, Li Y, Yan J, Hua Z, Chen H, Yan D, A new method for the synthesis of highly dispersive and catalytically active platinum nanoparticles confined in mesoporous zirconia. Adv Mater 2003;15:1078-1081.

[30] Fukuoka A, Araki H, Sakamoto Y, Sugimoto N, Tsukada H, Kumai Y, Akimoto Y, Ichikawa M, Template synthesis of nanoparticle arrays of gold and platinum in mesoporous silica films. Nano Lett., 2002, 2, 793-795.

[31] Vinu A, Hossain KZ, Ariga K. Recent advances in functionalization of mesoporous silica. J. Nanosci. Nanotech 2005; 5:347-371.

[32] Walcarius A, Etienne M, Lebeau B. Rate of access to the binding sites in organically modified silicates. 2. ordered mesoporous silicas grafted with amine or thiol groups. Chem Mater 2003; 15: 2161–2173.

[33] Walcarius A, Etienne M, Sayen S, Lebeau B. Grafted silicas in electroanalysis: amorphous versus ordered mesoporous materials. Electroanal 2003;15: 414-421.

[34] Khdary NH, Ghanem MA, Merajuddine MG, Bin Manie FM. Incorporation of Cu, Fe, Ag, and Au nanoparticles in mercapto-silica (MOS) and their CO_2 adsorption capacities. J CO_2 Utilization 2014; 5:17–23.

[35] Wieckowski A, Savinova E R, Vayenas CG. Catalysis and electrocatalysis at nanoparticle surfaces. New York; Marcel Dekker:2003.

[36] Chen A, Holt-Hindle P. Platinum-based nanostructured materials: Synthesis, properties, and applications. Chem Rev 2010; 110: 3767–3804.

[37] Khdary NH, Ghanem MA. Metal–organic–silica nanocomposites: copper, silver nanoparticles–ethylenediamine–silica gel and their CO_2 adsorption behaviour. J Mater Chem 2012; 22:12032-1208

[38] Wang Z, Liu Q, Yu J, Wu T, Wang G. Surface structure and catalytic behavior of silica-supported copper catalysts prepared by impregnation and sol–gel methods. Appl Catal A 2003; 239: 87-94.

[39] Coates J. in Interpretation of Infrared Spectra, A Practical Approach in Encyclopedia of Analytical Chemistry. Chichester; John Wiley & Sons Ltd:2000.

[40] Shriner R L, Hermann CKF, Morril TC, Curtin DY, Fuson RC. Systematic identification of organic compounds. New York; John Wiley & Sons:1998.

[41] Jaroniec C P, Kruk M, Jaroniec M, Sayari A. Tailoring Surface and Structural Properties of MCM-41 Silicas by Bonding Organosilanes. J. Phys. Chem. B, 1998,102, 5503- 5510.

[42] Alonso-Lemus I, Verde-Gómez Y, Álvarez-Contreras L, Platinum nanoparticles synthesis supported in mesoporous silica and its effect in MCM-41 lattice. Int J Electrochem Sci 2011; 6:4176 - 4187

[43] Eswaramoorthy M, Niwa S, Toba M, Shimada H, Raj A, Mizukami F. The conversion of methane with silica-supported platinum catalysts: the effect of catalyst preparation method and platinum particle size Catal Lett 2001; 71:55-61.

[44] Ham D J, Ganesan R, Lee J S, Tungsten carbide microsphere as an electrode for cathodic hydrogen volution from water. Int J Hydrogen Energy 2008; 33:6865-72.

[45] Ojani R, Valiollahi R, Raoof J-B, Energy 2014; 74: 871-876